Mathematical Models and Methods in Applied Sciences
Vol. 28, No. 8 (2018) 1453–1480

DOI: 10.1142/S0218202518500392

World Scientific
www.worldscientific.com

A posteriori error estimators for hierarchical B-spline discretizations

Annalisa Buffa

École Polytechnique Fédérale de Lausanne,
School of Basic Sciences, MATHICSE-MNS,
Lausanne, Switzerland

Istituto di Matematica Applicata e Tecnologie Informatiche,
'E. Magenes' (CNR), Pavia, Italy
annalisa.buffa@epfl.ch

Eduardo M. Garau*

Universidad Nacional del Litoral,
Consejo Nacional de Investigaciones,
Científicas y Técnicas,
FIQ, Santa Fe, Argentina
egarau@santafe-conicet.gov.ar

Received 31 May 2017
Revised 6 March 2018
Accepted 14 March 2018
Published 22 May 2018
Communicated by Y. Bazilevs

In this paper, we develop a function-based *a posteriori* error estimators for the solution of linear second-order elliptic problems considering hierarchical spline spaces for the Galerkin discretization. We obtain a global upper bound for the energy error over arbitrary hierarchical mesh configurations which simplifies the implementation of adaptive refinement strategies. The theory hinges on some weighted Poincaré-type inequalities where the B-spline basis functions are the weights appearing in the norms. Such inequalities are derived following the lines in [A. Veeser and R. Verfürth, Explicit upper bounds for dual norms of residuals, *SIAM J. Numer. Anal.* **47** (2009) 2387–2405], where the case of standard finite elements is considered. Additionally, we present numerical experiments that show the efficiency of the error estimators independently of the degree of the splines used for the discretization, together with an adaptive algorithm guided by these local estimators that yields optimal meshes and rates of convergence, exhibiting an excellent performance.

Keywords: *A posteriori* error estimators; adaptivity; hierarchical splines.

AMS Subject Classification: 65N30, 65D07, 65N50, 65N12, 65N15, 41A25

*Corresponding author

1. Introduction

The design of reliable and efficient *a posteriori* error indicators for guiding local refinement when solving numerically partial differential equations is essential, both for defining a robust and automatic adaptive procedure and for ensuring to find suitable approximations of the desired solution without exceeding the limits of available software and hardware.

The main idea behind *a posteriori* error estimation is to build a properly locally refined mesh in order to equidistribute the approximation error. Whereas for standard finite element methods, several intuitive ways of refining locally a mesh are clear and broadly analyzed, for isogeometric methods,[11,23] the development of efficient and robust strategies to get suitably locally refined meshes constitutes a challenging problem because the tensor product structure of B-splines[13,31] is broken. Different alternatives have been proposed in order to tackle this situation, such as hierarchical splines,[26,38] T-splines,[4,32] or LR-splines.[6,14] Among them, hierarchical splines based on the construction presented in Ref. 38 are probably the easiest to define and to implement for their use in the context of isogeometric methods. In addition, several quasi-interpolation operators onto hierarchical spaces have been proposed[7,33,34] demonstrating their ability for local approximation.

A posteriori error estimation has been widely studied in the context of classical finite element methods (see Refs. 1 and 37, and the references therein) whereas adaptivity in isogeometric analysis using T-splines has been addressed in the pioneering paper.[15]

Recovery-based error estimators have been tested in Refs. 27 and 28, and refinement is achieved by LR B-splines. Moreover, functional based error estimators were proposed in Ref. 25, but without a real local refinement strategy behind.

Recently, some recovery-based error estimators using hierachical T-meshes have been proposed.[2] On the other hand, regarding the context of isogeometric boundary element methods (IGABEM) in 2D, some a posteriori error estimations have been developed in Ref. 17 and the linear convergence with optimal rates for an associated adaptive scheme has been proved in Ref. 16.

Furthermore, we mention Ref. 8, where residual based error indicators for hierarchical spline spaces have been proposed. In that case, the authors considered an approach following the standard techniques in classical finite elements for deriving element-based a posteriori error estimators using the truncated basis for hierarchical splines introduced in Refs. 21 and 22. The presented proof for the reliability of such estimators needs to assume some restrictions over the hierarchical meshes, with the purpose of controlling the overlap of the truncated basis function supports. More recently, in Ref. 19 the authors claim optimal convergence rates for an adaptive algorithm guided by element-based local error indicators like the ones in Ref. 8, although they assume stronger restrictions over the hierarchical mesh configurations.

We note that although truncation is indeed a possible strategy to recover partition of unity, this procedure requires a specific construction that entails complicated basis function supports, that may be non-convex and/or not connected, and their use may produce a non-negligible overhead with an adaptive strategy. Thus, in this paper, we consider the hierarchical basis without truncation recovering the simplicity of basis function supports, that in this case are boxes. Moreover, taking into account the hierarchical space defined in Ref. 7, we can also recover the partition of unity.

The main goal of this paper is to obtain simple residual-type *a posteriori* error estimators for linear second-order elliptic problems using discretizations in hierarchical spline spaces. As pointed out in Ref. 7, where the hierarchical basis can be obtained simply through parent–children relations, the design of estimators associated to basis functions (instead of elements) seems to be more suitable for guiding adaptive refinements. We derive reliable function-based *a posteriori* error indicators without any restrictions over the hierarchical mesh configurations, i.e. we are able to bound the error in energy norm by our global a posteriori error indicator. As we mentioned above, the *a posteriori* error analysis with hierarchical splines presented in the existent literature has been always based on local error indicators associated to the elements in the mesh. We think that the approach based on error estimators associated to the basis functions of the discrete space is more natural in the context of splines and suitable for the design of adaptive refinement techniques (see also Refs. 38 and 24) since we can indeed guarantee a higher local resolution by refining supports of basis functions unlike what happens if we refine only isolated elements. Moreover, having no restrictions on the considered hierarchical meshes simplifies the implementation of adaptive refinement because we do not have to enforce any artificial and supplementary refinement in order to preserve an admissibility criterion on the adaptive meshes.

The proof of the reliability of our *a posteriori* error estimators relies on some Poincaré-type inequalities where the B-splines are considered as weight functions taking advantage of the fact that their supports are, obviously, convex sets. More generally, our approach can be considered as a generalization to high order splines of some existent Poincaré-type inequalities. Although we follow closely the lines from Ref. 36, where specific Poincaré-type inequalities are proved and the classical barycentric coordinate functions appear as weight functions, we emphasize that our analysis represents a major difference compared to standard finite element techniques. Additionally, it is important to mention that in Ref. 29, similar inequalities had already been stated for deriving *a posteriori* error estimators for standard finite element discretizations of symmetric linear elliptic problems, but in that case, the error estimators were defined by solving some local problems on stars.

This paper is organized as follows. In Sec. 2, we briefly introduce the variational formulation of the elliptic problem that we consider, and in Sec. 3, we describe precisely the hierarchical spline spaces that we use for its Galerkin discretization.

Next, we state and prove some Poincaré-type inequalities that have B-splines as weight functions in Sec. 4, which are used in Sec. 5 to derive function-based *a posteriori* error estimators and to prove that such estimators constitute an upper bound for the energy error. In Sec. 6, we analyze a reduction property of our estimators after refinement of the hierarchical mesh. Finally, in Sec. 7, we propose an adaptive algorithm guided by our estimators and illustrate its behavior through several numerical tests, showing that the global estimator is efficient and the algorithm experimentally converges with the optimal rate.

2. Problem Setting

For simplicity, we consider the following linear elliptic problem on the parametric domain $\Omega = [0,1]^d \subset \mathbb{R}^d$, $d = 2, 3, \ldots,$

$$\begin{cases} -\operatorname{div}(\mathcal{A}\nabla u) + \boldsymbol{b}\cdot\nabla u + cu = f & \text{in } \Omega, \\ u = 0 & \text{on } \partial\Omega, \end{cases} \tag{2.1}$$

where $\mathcal{A} \in W^{1,\infty}(\Omega;\mathbb{R}^{d\times d})$ is uniformly symmetric positive definite over Ω, i.e. there exist constants $0 < \gamma_1 \le \gamma_2$ such that

$$\gamma_1|\xi|^2 \le \xi^T\mathcal{A}(x)\xi \le \gamma_2|\xi|^2, \quad \forall\, x \in \Omega,\ \ \xi \in \mathbb{R}^d, \tag{2.2}$$

$\boldsymbol{b} \in L^\infty(\Omega) \cap H(\operatorname{div},\Omega)$, $c \in L^\infty(\Omega)$. We assume that $c - \frac{1}{2}\operatorname{div}\boldsymbol{b} \ge 0$.

We say that $u \in H_0^1(\Omega) := W_0^{1,2}(\Omega)$ is a weak solution of (2.1) if

$$B[u,v] = F(v), \quad \forall\, v \in H_0^1(\Omega), \tag{2.3}$$

where $B : H_0^1(\Omega)\times H_0^1(\Omega) \to \mathbb{R}$ is the bounded bilinear form given by

$$B[u,v] := \int_\Omega \mathcal{A}\nabla u\cdot\nabla v + \boldsymbol{b}\cdot\nabla u\, v + c\,u\,v,$$

and $F : H_0^1(\Omega) \to \mathbb{R}$ is the linear functional defined by

$$F(v) := \int_\Omega fv.$$

Taking into account (2.2) and that $c - \frac{1}{2}\operatorname{div}(\boldsymbol{b}) \ge 0$, it is easy to check that B is coercive, that is,

$$\gamma_1\|\nabla v\|^2_{L^2(\Omega)} \le B[v,v], \quad \forall\, v \in H_0^1(\Omega). \tag{2.4}$$

Thus, as a consequence of the Lax–Milgram theorem, we have that problem (2.3) is well posed.

3. Discretization Using Hierarchical Spline Spaces

In this section, we revise briefly the definitions of univariate and tensor product B-splines that we use to build a basis for a hierarchical spline space like those from Refs. 26 and 38. Then, we state the discrete formulation of problem (2.3) when considering such spaces.

3.1. *Univariate B-spline bases*

Let $\Xi_{p,n} := (\xi_j)_{j=1}^{n+p+1}$ be a p-open knot vector, i.e. a *sequence* such that

$$0 = \xi_1 = \cdots = \xi_{p+1} < \xi_{p+2} \leq \cdots \leq \xi_n < \xi_{n+1} = \cdots = \xi_{n+p+1} = 1,$$

where the two positive integers p and n denote a given polynomial degree, and the corresponding number of B-splines defined over the subdivision $\Xi_{p,n}$, respectively. Here, $n \geq p+1$. We also introduce the *set* $Z_{p,n} := \{\zeta_j\}_{j=1}^{\widetilde{n}}$ of breakpoints (i.e. knots without repetitions), and denote by m_j the multiplicity of the breakpoint ζ_j, such that

$$\Xi_{p,n} = (\underbrace{\zeta_1, \ldots, \zeta_1}_{m_1 \text{ times}}, \underbrace{\zeta_2, \ldots, \zeta_2}_{m_2 \text{ times}}, \ldots \underbrace{\zeta_{\widetilde{n}}, \ldots, \zeta_{\widetilde{n}}}_{m_{\widetilde{n}} \text{ times}}),$$

with $\sum_{i=1}^{\widetilde{n}} m_i = n+p+1$. Note that the two extreme knots are repeated $p+1$ times, i.e. $m_1 = m_{\widetilde{n}} = p+1$. We assume that an internal knot can be repeated at most $p+1$ times, that is, $m_j \leq p+1$, for $j = 2, \ldots, \widetilde{n}-1$.

Let $\mathcal{B}(\Xi_{p,n}) := \{b_1, b_2, \ldots, b_n\}$ be the B-spline basis[13,31] associated to the knot vector $\Xi_{p,n}$. In particular, we remark that the *local knot vector* of b_j is given by $(\xi_j, \ldots, \xi_{j+p+1})$, which is a subsequence of $p+2$ consecutive knots of $\Xi_{p,n}$; and that the support of b_j, denoted by $\operatorname{supp} b_j$, is the closed interval $[\xi_j, \xi_{j+p+1}]$. Additionally, the B-spline basis $\mathcal{B}(\Xi_{p,n})$ is in fact a basis for the space $\mathcal{S}_{p,n}$ of the piecewise polynomials of degree p over the mesh $\mathcal{I}(\Xi_{p,n}) := \{[\zeta_j, \zeta_{j+1}] \,|\, j = 1, \ldots, \widetilde{n}-1\}$ that have $r_j := p - m_j$ continuous derivatives at the breakpoint ζ_j, for $j = 1, \ldots, \widetilde{n}$. If $r_j = -1$ for some j, the splines in $\mathcal{S}_{p,n}$ can be discontinuous at ζ_j.

3.2. *Tensor product B-spline bases*

Let $d \geq 1$. In order to define a tensor product d-variate spline function space on the parametric domain $\Omega := [0,1]^d \subset \mathbb{R}^d$, we consider $\mathbf{p} := (p_1, p_2, \ldots, p_d)$ the vector of polynomial degrees with respect to each coordinate direction and $\mathbf{n} := (n_1, n_2, \ldots, n_d)$, where $n_i \geq p_i + 1$. For $i = 1, 2, \ldots, d$, let $\Xi_{p_i,n_i} := (\xi_j^{(i)})_{j=1}^{n_i+p_i+1}$ be a p_i-open knot vector, i.e.

$$0 = \xi_1^{(i)} = \cdots = \xi_{p_i+1}^{(i)} < \xi_{p_i+2}^{(i)} \leq \cdots \leq \xi_{n_i}^{(i)} < \xi_{n_i+1}^{(i)} = \cdots = \xi_{n_i+p_i+1}^{(i)} = 1,$$

where the two extreme knots are repeated p_i+1 times and any internal knot can be repeated at most p_i+1 times. We denote by $\mathcal{S}_{\mathbf{p},\mathbf{n}}$ the tensor product spline space spanned by the B-spline basis $\mathcal{B}_{\mathbf{p},\mathbf{n}}$ defined as the tensor product of the univariate B-spline bases $\mathcal{B}(\Xi_{p_1,n_1}), \ldots, \mathcal{B}(\Xi_{p_d,n_d})$. More precisely, $\beta \in \mathcal{B}_{\mathbf{p},\mathbf{n}}$ if and only if

$$\beta(x) = \beta_1(x_1) \ldots \beta_j(x_j) \ldots \beta_d(x_d), \tag{3.1}$$

where $\beta_j \in \mathcal{B}(\Xi_{p_j,n_j})$, for $j = 1, 2, \ldots, d$, and x_j denotes the jth component of $x \in \mathbb{R}^d$. We note that the support of β, denoted by ω_β, is a box in $\mathbb{R}^d$ given by

$$\omega_\beta := \operatorname{supp} \beta = \operatorname{supp} \beta_1 \times \cdots \times \operatorname{supp} \beta_j \times \cdots \times \operatorname{supp} \beta_d. \tag{3.2}$$

Finally, the associated Cartesian grid $\mathcal{Q}_{\mathbf{p},\mathbf{n}}$ consists of the cells $Q = I_1 \times \cdots \times I_d$, where I_i is an element (closed interval) of the ith univariate mesh $\mathcal{I}(\Xi_{p_i,n_i})$, for $i = 1, \ldots, d$.

3.3. *Sequence of tensor product spline spaces*

In order to define a hierarchical structure, we assume that there exists an underlying sequence of tensor product d-variate spline spaces $\{\mathcal{S}_\ell\}_{\ell \in \mathbb{N}_0}$, where $\mathcal{S}_\ell$ is called *the space of level* ℓ, such that

$$\mathcal{S}_0 \subset \mathcal{S}_1 \subset \mathcal{S}_2 \subset \mathcal{S}_3 \subset \cdots. \tag{3.3}$$

Each of these spaces are indeed obtained from a tensorization of univariate spline spaces as we explain now.

Let $\mathbf{p} := (p_1, p_2, \ldots, p_d)$ denote the chosen vector of polynomial degrees for the univariate splines in each coordinate direction. For $\ell \in \mathbb{N}_0$, $\mathcal{S}_\ell := \mathcal{S}_{\mathbf{p},\mathbf{n}_\ell}$ is the tensor product spline space and $\mathcal{B}_\ell := \mathcal{B}_{\mathbf{p},\mathbf{n}_\ell}$ is the corresponding B-spline basis, that we call the set of *B-splines of level* ℓ, for some $\mathbf{n}_\ell = (n_1^{(\ell)}, n_2^{(\ell)}, \ldots, n_d^{(\ell)})$. In order to guarantee (3.3), we assume that if ξ is a knot in $\Xi_{p_i,n_i^{(\ell)}}$ with multiplicity m, then ξ is also a knot in $\Xi_{p_i,n_i^{(\ell+1)}}$ with multiplicity at least m, for $i = 1, \ldots, d$ and $\ell \in \mathbb{N}_0$. Furthermore, we denote by $\mathcal{Q}_\ell := \mathcal{Q}_{\mathbf{p},\mathbf{n}_\ell}$ the corresponding Cartesian mesh, and we say that $Q \in \mathcal{Q}_\ell$ is a *cell of level* ℓ. We note that we assume that the cells are closed sets.

B-splines possess several important properties, such as non-negativity, partition of unity, local linear independence and local support, that make them suitable for design and analysis, see Refs. 11, 13 and 31 for details. Moreover, we have that B-splines of level ℓ can be written as linear combinations of B-splines of level $\ell+1$ with non-negative coefficients, which is known as *two-scale relation*. More specifically, if $\mathcal{B}_\ell = \{\beta_{i,\ell} \mid i = 1, \ldots, N_\ell\}$, where N_ℓ is the dimension of the space $\mathcal{S}_\ell$, for $\ell \in \mathbb{N}_0$; this property can be stated as follows:

$$\beta_{i,\ell} = \sum_{k=1}^{N_{\ell+1}} c_{k,\ell+1}(\beta_{i,\ell})\, \beta_{k,\ell+1}, \quad \forall\, \beta_{i,\ell} \in \mathcal{B}_\ell \tag{3.4}$$

with $c_{k,\ell+1}(\beta_{i,\ell}) \geq 0$. We note that, due to the local linear independence of B-splines, only a limited number of the coefficients $c_{k,\ell+1}(\beta_{i,\ell})$ are different from zero. Taking into account (3.4), the set of children of $\beta_{i,\ell}$, denoted by $\mathcal{C}(\beta_{i,\ell})$, is defined by

$$\mathcal{C}(\beta_{i,\ell}) := \{\beta_{k,\ell+1} \in \mathcal{B}_{\ell+1} \mid c_{k,\ell+1}(\beta_{i,\ell}) \neq 0\}.$$

As we will see later on, in cases of interest such as subsequent levels obtained by dyadic refinement, the number of children is bounded and it depends solely on the degree $\mathbf{p}$.

3.4. *Hierarchical spline space*

In Ref. 7, the authors considered a particular subspace of the hierarchical space presented in Refs. 26 and 38, which still enjoys good local approximation properties

and leads to simple refinement schemes, because it is defined in a way that focuses on the relation between functions. Although throughout this work, we consider the hierarchical space as defined in Ref. 7 because we consider that this definition is simpler and more natural for adaptive purposes, we note that all the results to be stated in Secs. 5 and 6 hold when the hierarchical space as defined in Ref. 38 is considered. In order to define precisely a basis for the hierarchical space that we consider, we first need to fix a hierarchy of subdomains of $\Omega = [0,1]^d$ as in the next definition, which in turn provides the different levels in the multilevel structure.

Definition 3.1. (Hierarchy of subdomains) Let $n \in \mathbb{N}$ be arbitrary. We say that the set $\mathbf{\Omega}_n := \{\Omega_0, \Omega_1, \dots, \Omega_n\}$ is a hierarchy of subdomains of Ω of depth n if

$$\Omega = \Omega_0 \supset \Omega_1 \supset \cdots \supset \Omega_{n-1} \supset \Omega_n = \varnothing,$$

and each subdomain Ω_ℓ is the union of cells of level $\ell - 1$, for $\ell = 1, \dots, n-1$.

We now are in the position of introducing the basis for the hierarchical space.

Definition 3.2. (Hierarchical basis) Let $\{\mathcal{S}_\ell\}_{\ell \in \mathbb{N}_0}$ be a sequence of spaces like (3.3) with the corresponding B-spline bases $\{\mathcal{B}_\ell\}_{\ell \in \mathbb{N}_0}$, and $\mathbf{\Omega}_n := \{\Omega_0, \Omega_1, \dots, \Omega_n\}$ a hierarchy of subdomains of depth n. We define the *hierarchical basis* $\mathcal{H} := \mathcal{H}_{n-1}$ computed with the following recursive algorithm:

$$\begin{cases} \mathcal{H}_0 := \mathcal{B}_0, \\ \mathcal{H}_{\ell+1} := \{\beta \in \mathcal{H}_\ell \,|\, \operatorname{supp} \beta \not\subset \Omega_{\ell+1}\} \cup \displaystyle\bigcup_{\substack{\beta \in \mathcal{H}_\ell \\ \operatorname{supp} \beta \subset \Omega_{\ell+1}}} \mathcal{C}(\beta), \quad \ell = 0, \dots, n-2. \end{cases}$$

An interesting property of the hierarchical basis $\mathcal{H}$ is that the coefficients for writing the unity are strictly positive. That is, we have

$$\sum_{\beta \in \mathcal{H}} a_\beta \beta(x) = 1, \quad \text{for } x \in \Omega \tag{3.5}$$

with $a_\beta > 0$ (see Theorem 5.2 in Ref. 7).

In the following, we say that β is an *active function* if $\beta \in \mathcal{H}$, it is an *active function of level* ℓ if $\beta \in \mathcal{H} \cap \mathcal{B}_\ell$, and it is a *deactivated function of level* ℓ if $\beta \in \mathcal{H}_\ell \setminus \mathcal{H}_{\ell+1}$. Moreover, $\mathcal{H}_\ell \cap \mathcal{B}_\ell$ is the set of active and deactivated functions of level ℓ.

We remark that, unlike the definition given in Ref. 38 where a B-spline of level $\ell+1$ is added to $\mathcal{H}_{\ell+1}$ if its support is contained in $\Omega_{\ell+1}$, in Definition 3.2, B-splines of level $\ell+1$ are added only if they are children of a deactivated function of level ℓ. Furthermore, when considering the basis from Ref. 38, some coefficients for writing the unity as in (3.5) can be indeed equal to zero.

The hierarchical spline basis $\mathcal{H}$ is associated to an underlying *hierarchical mesh* $\mathcal{Q} \equiv \mathcal{Q}(\mathbf{\Omega}_n)$, given by

$$\mathcal{Q} := \bigcup_{\ell=0}^{n-1} \{Q \in \mathcal{Q}_\ell \,|\, Q \subset \Omega_\ell \wedge Q \not\subset \Omega_{\ell+1}\}.$$

Analogously, we say that Q is an *active cell* if $Q \in \mathcal{Q}$, and it is an *active cell of level* ℓ if $Q \in \mathcal{Q}_\ell \cap \mathcal{Q}$. We will also say that Q is a *deactivated cell of level* ℓ if $Q \in \mathcal{Q}_\ell$ and $Q \subset \Omega_{\ell+1}$.

Finally, we note that a B-spline of level ℓ is active if all the active cells within its support are of level ℓ or higher, and at least one of such cells is actually of level ℓ. A B-spline is deactivated when all the cells of its level within the support are deactivated.

3.5. *Discretization of the variational problem*

In order to discretize problem (2.3), we consider a hierarchy of subdomains Ω_n of Ω and the corresponding spline space $\mathcal{S}(\mathcal{Q}) := \operatorname{span} \mathcal{H}$ with the hierarchical basis $\mathcal{H}$ and the mesh $\mathcal{Q}$ as defined above. Now, we define the discrete space $\mathcal{S}_0 \equiv \mathcal{S}_0(\mathcal{Q})$ by

$$\mathcal{S}_0 := \{V \in \mathcal{S}(\mathcal{Q}) \,|\, V_{|\partial\Omega} \equiv 0\}.$$

Thus, the discrete counterpart of (2.3) consists in finding $U \in \mathcal{S}_0$ such that

$$B[U, V] = F(V), \quad \forall\, V \in \mathcal{S}_0. \tag{3.6}$$

4. Weighted Poincaré-type Inequalities

In this section, we briefly revise some basic notions about weighted Sobolev spaces and then we state weighted Poincaré-type inequalities (see Theorems 4.1 and 4.3) that will be needed for proving the reliability of the function-based *a posteriori* error estimators to be presented in the next section.

4.1. *Some definitions about weighted Sobolev spaces*

Let $A \subset \mathbb{R}^d$ be a bounded domain with Lipschitz boundary. If ρ is a non-negative locally integrable function, we denote by $L^2(A, \rho)$ the space of measurable functions u such that

$$\|u\|_{L^2(A,\rho)} := \left(\int_A |u(x)|^2 \rho(x) dx \right)^{\frac{1}{2}} < \infty.$$

Note that $L^2(A, \rho)$ is a Hilbert space equipped with the scalar product

$$\langle u, v \rangle_{A,\rho} := \int_A u(x) v(x) \rho(x) dx.$$

We also define the weighted Sobolev space $H^1(A, \rho)$ of weakly differentiable functions u such that $\|u\|_{H^1(A,\rho)} < \infty$, where

$$\|u\|^2_{H^1(A,\rho)} := \|u\|^2_{L^2(A,\rho)} + \|\nabla u\|^2_{L^2(A,\rho)}.$$

Finally, $H^1_0(A, \rho)$ is the closure of $C^\infty_0(A)$ in $H^1(A, \rho)$.

4.2. *A weighted Poincaré inequality*

Before stating the main result of this section, we recall the definition of concave functions.

Definition 4.1. (Concave function) A function f defined on a convex set $A \subset \mathbb{R}^d$ is *concave on* A if for any α, $0 < \alpha < 1$, there holds

$$f(\alpha x + (1-\alpha)y) \geq \alpha f(x) + (1-\alpha) f(y), \quad \forall\, x, y \in A.$$

The weighted Poincaré inequality stated in Ref. 10 holds for weights ρ such that ρ^s is a concave function on its support, for some $s > 0$. Thus, in view of Theorem 4.2, which states that this is the case when ρ is a multivariate B-spline basis function, the following result is an immediate consequence of Theorems 1.1 and 1.2 in Ref. 10 (see also Lemma 5.2 in Ref. 36).

Theorem 4.1. (*Weighted Poincaré inequality*) *If β is a tensor product B-spline basis function, then*

$$\|v - c_\beta\|_{L^2(\omega_\beta,\beta)} \leq \frac{1}{\pi} \operatorname{diam}(\omega_\beta) \|\nabla v\|_{L^2(\omega_\beta,\beta)}, \quad \forall\, v \in H^1(\omega_\beta, \beta),$$

where $c_\beta := \dfrac{\int_{\omega_\beta} v\,\beta}{\int_{\omega_\beta} \beta}$ *and* $\omega_\beta := \operatorname{supp} \beta$.

In order to prove that β^s is a concave function on its support, for some $s > 0$, when β is a tensor product B-spline basis function, we first note that the result holds for univariate B-splines thanks to the Brunn–Minkowski inequality, as explained in Sec. 2 in Ref. 12. More precisely, the following result holds.

Lemma 4.1. *Let β be a univariate B-spline basis function of degree p. Then, $\beta^{\frac{1}{p}}$ is concave on its support.*

The following *generalized Cauchy–Schwarz inequality* can be proved by mathematical induction:

$$(a_1^d + b_1^d)^{\frac{1}{d}} (a_2^d + b_2^d)^{\frac{1}{d}} \cdots (a_d^d + b_d^d)^{\frac{1}{d}} \geq a_1 a_2 \ldots a_d + b_1 b_2 \ldots b_d, \tag{4.1}$$

for all non-negative numbers $a_1, a_2, \ldots, a_d, b_1, b_2, \ldots, b_d$.

Now, as a consequence of (4.1), we have the following result.

Lemma 4.2. *If $f_1, f_2, \ldots, f_d$ are non-negative concave functions on a convex set $A \subset \mathbb{R}^d$ then $(f_1 f_2 \cdots f_d)^{\frac{1}{d}}$ is concave on A.*

Proof. In view of Definition 4.1, the assertion of this lemma follows from (4.1) taking $a_i = (\alpha f_i(x))^{\frac{1}{d}}$ and $b_i = ((1-\alpha) f_i(y))^{\frac{1}{d}}$, for $i = 1, \ldots, d$. □

Finally, using Lemma 4.1 and the last lemma, we can prove the following result.

Theorem 4.2. *Let β be a tensor product d-variate B-spline basis function as in* (3.1)*. If the univariate B-splines that define β are of degree p, then $\beta^{\frac{1}{pd}}$ is concave on its support.*

Proof. From (3.1), we have that $\beta(x) = \beta_1(x_1) \cdots \beta_j(x_j) \cdots \beta_d(x_d)$, where β_j are univariate B-splines, for $j = 1, 2, \ldots, d$, and x_j denotes the jth component of $x \in \mathbb{R}^d$.

Now, by Lemma 4.1, we have that $f_j(x) := \beta_j(x_j)^{\frac{1}{p}}$ is concave, for $j = 1, 2, \ldots, d$. Finally, applying Lemma 4.2, we obtain that $(\beta_1(x_1)^{\frac{1}{p}} \ldots \beta_j(x_j)^{\frac{1}{p}} \ldots \beta_d(x_d)^{\frac{1}{p}})^{\frac{1}{d}} = \beta(x)^{\frac{1}{pd}}$ is concave on its support. □

4.3. *A weighted Friedrichs inequality*

When considering Dirichlet boundary conditions as in problem (2.1), it is useful to have a suitable weighted Poincaré–Friedrichs inequality in the case that the weight function is a B-spline which does not vanish on a part of the boundary of Ω. More precisely, we have the following result, which generalizes Lemma 5.1 in Ref. 36 to high order splines.

Theorem 4.3. (*Weighted Friedrichs inequality*) *Let β be a tensor product B-spline basis function such that $\beta_{|\partial\Omega} \not\equiv 0$. Then, there exists a constant $C_F > 0$, independent of β, such that*

$$\|v\|_{L^2(\omega_\beta,\beta)} \leq C_F \operatorname{diam}(\omega_\beta) \|\nabla v\|_{L^2(\omega_\beta,\beta)}, \tag{4.2}$$

for all $v \in H^1(\omega_\beta, \beta)$ satisfying $v_{|\Gamma_\beta} \equiv 0$, where $\Gamma_\beta := \partial\Omega \cap \partial\omega_\beta$ is a set with positive $(d-1)$-dimensional Lebesgue measure and $\omega_\beta := \operatorname{supp}\beta$. More precisely, the constant C_F depends on the polynomial degree p, the dimension d, and $\frac{\max \operatorname{diam}(Q)}{\min \operatorname{diam}(Q)}$, where the maximum and minimum are taken over all cells Q in the associated Cartesian grid.

The Friedrichs inequality stated in the last theorem can be proved following the same steps from Ref. 36. In particular, such inequality can be obtained as a consequence of the weighted Poincaré inequality given in Theorem 4.1 and a suitable weighted trace inequality.

The following result is a trace theorem where B-splines are used as weight functions and can be seen as an extension of Proposition 4.3 in Ref. 36; its proof follows exactly the same lines, but we include it here to make this article more self-contained.

Proposition 4.1. (*Weighted trace theorem*) *Let β be a tensor product B-spline basis function given by*

$$\beta(x) = \beta_1(x_1) \cdots \beta_j(x_j) \cdots \beta_d(x_d),$$

where β_j are univariate B-splines of a fixed degree p, for $j = 1, 2, \ldots, d$, and x_j denotes the jth component of $x \in \mathbb{R}^d$. Assume that $\beta_{|\partial\Omega} \not\equiv 0$, and let $Q \subset \operatorname{supp}\beta$ be a cell of the associated Cartesian grid that has a side $S \subset \partial\Omega$ such that $\beta_{|S} \not\equiv 0$. Then,

$$\frac{\int_S w\beta}{\int_S \beta} - \frac{\int_Q w\beta}{\int_Q \beta} = \frac{1}{p+1} \frac{\int_Q \gamma_{Q,S} \cdot \nabla w \, \beta}{\int_Q \beta}, \quad \forall\, w \in W^{1,1}(Q), \tag{4.3}$$

where $\gamma_{Q,S}(x) := (x_i - a_i)\mathbf{e}_i$, for $x = (x_1, \ldots, x_d) \in Q$. Here, $a = (a_1, \ldots, a_d)$ is any vertex of Q that does not belong to S and i denotes the coordinate direction given by the unit vector $\mathbf{e}_i$ that is orthogonal to the side S.

Proof. In this proof, we use the symbol $\fint_A f$ to denote the average of a function f over a set A, that is, $\frac{1}{|A|}\int_A f$.

If $v \in W^{1,1}(Q)$, as an immediate consequence of Gauss divergence theorem (see also Proposition 4.2 in Ref. 36) to the vector field $v\gamma_{Q,S}$, it follows that

$$\fint_S v - \fint_Q v = \fint_Q \gamma_{Q,S} \cdot \nabla v. \tag{4.4}$$

Now, let $w \in W^{1,1}(Q)$. Applying (4.4) with $v = w\beta$, we obtain

$$\fint_S w\beta - \fint_Q w\beta = \fint_Q \gamma_{Q,S} \cdot \nabla(w\beta) = \fint_Q \gamma_{Q,S} \cdot \nabla w\, \beta + \fint_Q \gamma_{Q,S} \cdot \nabla \beta\, w. \tag{4.5}$$

Let i be the coordinate direction given by the unit vector $\mathbf{e}_i$ that is orthogonal to the side S. Taking into account that $\beta_{|_S} \not\equiv 0$ and that $S \subset \partial\Omega$, we have that $\beta_i(x_i) = \frac{|S|^p}{|Q|^p}|x_i - a_i|^p$, where $a = (a_1, \ldots, a_d)$ is any vertex of Q that does not belong to S, which in turn implies that

$$\gamma_{Q,S}(x) \cdot \nabla\beta(x) = p\beta(x), \quad \forall\, x \in Q.$$

Thus, from (4.5), we obtain that

$$\fint_S w\beta - (p+1)\fint_Q w\beta = \fint_Q \gamma_{Q,S} \cdot \nabla w\, \beta.$$

Finally, (4.3) follows from the last equation dividing both sides by $\int_S \beta$, and taking into account that $\fint_S \beta = (p+1)\fint_Q \beta$. □

We finish this section using the last proposition for proving the weighted Friedrichs inequality stated in Theorem 4.3.

Proof of Theorem 4.3. Let β be a tensor product B-spline basis function such that $\beta_{|_{\partial\Omega}} \not\equiv 0$ and let $Q \subset \operatorname{supp}\beta$ be a cell of the associated Cartesian grid that has a side $S \subset \partial\Omega$ such that $\beta_{|_S} \not\equiv 0$. Then, for all $c \in \mathbb{R}$ and $v \in H^1(\omega_\beta, \beta)$ such that $v_{|_{\Gamma_\beta}} \equiv 0$, we have that

$$\begin{aligned}\|v\|_{L^2(\omega_\beta,\beta)} &\le \|v - c\|_{L^2(\omega_\beta,\beta)} + \|c\|_{L^2(\omega_\beta,\beta)} \\ &= \|v - c\|_{L^2(\omega_\beta,\beta)} + \left(\int_{\omega_\beta} \beta\right)^{\frac{1}{2}} \frac{\int_S |v-c|\beta}{\int_S \beta},\end{aligned} \tag{4.6}$$

where in the last equality, we have used that $S \subset \Gamma_\beta$. Now, applying Proposition 4.1 with $w = |v - c|$, taking into account that $\max_{x\in Q}|\gamma_{Q,S}(x)| \le \frac{|Q|}{|S|}$ and using Hölder inequality, we have

$$\begin{aligned}\frac{\int_S |v-c|\beta}{\int_S \beta} &\le \frac{\int_Q |v-c|\beta}{\int_Q \beta} + \frac{1}{p+1}\frac{|Q|}{|S|}\frac{\int_Q |\nabla v|\beta}{\int_Q \beta} \\ &\le \frac{1}{(\int_Q \beta)^{\frac{1}{2}}}\left(\|v - c\|_{L^2(Q,\beta)} + \frac{1}{p+1}\frac{|Q|}{|S|}\|\nabla v\|_{L^2(Q,\beta)}\right).\end{aligned}$$

If we use the last inequality to bound the second term in the right-hand side of (4.6), we obtain

$$\|v\|_{L^2(\omega_\beta,\beta)} \le \|v-c\|_{L^2(\omega_\beta,\beta)} + \left(\frac{\int_{\omega_\beta}\beta}{\int_Q \beta}\right)^{\frac{1}{2}} \left(\|v-c\|_{L^2(\omega_\beta,\beta)} + \frac{\operatorname{diam}(\omega_\beta)}{p+1}\|\nabla v\|_{L^2(\omega_\beta,\beta)}\right).$$

Finally, taking into account Theorem 4.1, we have that

$$\|v\|_{L^2(\omega_\beta,\beta)} \le \left(\frac{1}{\pi} + \left(\frac{\int_{\omega_\beta}\beta}{\int_Q \beta}\right)^{\frac{1}{2}} \left(\frac{1}{\pi} + \frac{1}{p+1}\right)\right) \operatorname{diam}(\omega_\beta)\|\nabla v\|_{L^2(\omega_\beta,\beta)},$$

which in turn implies (4.2). □

5. A Computable Upper Bound for the Error

In this section, we use the Poincaré-type inequalities proved in the previous section in order to get an *a posteriori* upper bound for the energy error when computing the discrete solution of problem (2.3) using the hierarchical schemes proposed in Sec. 3. Once such key inequalities are available, the procedure to derive reliable residual-type *a posteriori* error estimators follows the standard steps used when considering classical finite elements.

Let $u \in H_0^1(\Omega)$ be the solution of problem (2.3) and $U \in \mathcal{S}_0$ be the Galerkin approximation of u satisfying (3.6). Specifically, the main goal of this section is to define some computable quantities $\mathcal{E}_{\mathcal{H}}(U,\beta)$, for $\beta \in \mathcal{H}$, so that

$$\|\nabla(u-U)\|_{L^2(\Omega)} \le C\left(\sum_{\beta\in\mathcal{H}} \mathcal{E}_{\mathcal{H}}(U,\beta)^2\right)^{\frac{1}{2}},$$

for some constant $C > 0$.

Note that the coercivity (2.4) of the bilinear form implies that

$$\|\nabla(u-U)\|^2_{L^2(\Omega)} \le \frac{1}{\gamma_1} B[u-U,u-U] = \frac{1}{\gamma_1}\langle \mathbf{R}(U), u-U\rangle,$$

where the *residual* $\mathbf{R}$ of a function $V \in \mathcal{S}_0$ is given by

$$\langle \mathbf{R}(V), v\rangle := F(v) - B[V,v] = B[u-V,v], \quad \text{for all } v \in H_0^1(\Omega).$$

Thus, we have that

$$\|\nabla(u-U)\|_{L^2(\Omega)} \le \frac{1}{\gamma_1}\|\mathbf{R}(U)\|_{H^{-1}(\Omega)}, \tag{5.1}$$

and therefore, we have to bound $\|\mathbf{R}(U)\|_{H^{-1}(\Omega)}$. Assuming that $\mathcal{S}_0 \subset C^1(\Omega)$, since $U \in \mathcal{S}_0$, integration by parts yields

$$\langle \mathbf{R}(U), v\rangle = \int_\Omega \underbrace{(f + \operatorname{div}(\mathcal{A}\nabla U) - \boldsymbol{b}\cdot\nabla U - cU)}_{=:r(U)} v, \quad \forall\, v \in H_0^1(\Omega).$$

Now, for each $v \in H_0^1(\Omega)$, we associate a discrete function $v_{\mathcal{Q}} \in \mathcal{S}_0$ given by

$$v_{\mathcal{Q}} := \sum_{\beta \in \mathcal{H}} c_\beta a_\beta \beta, \quad \text{where } c_\beta := \begin{cases} \dfrac{\int_{\omega_\beta} v\beta}{\int_{\omega_\beta} \beta} & \text{if } \beta_{|\partial\Omega} \equiv 0, \\ 0 & \text{otherwise.} \end{cases}$$

Here, the coefficients a_β are those given by (3.5) and $\omega_\beta = \operatorname{supp} \beta$ (cf. (3.2)). Taking into account that $\sum_{\beta \in \mathcal{H}} a_\beta \beta \equiv 1$ on Ω and using that U satisfies (3.6), we have that

$$\langle \mathbf{R}(U), v \rangle = \langle \mathbf{R}(U), v - v_{\mathcal{Q}} \rangle = \sum_{\beta \in \mathcal{H}} a_\beta \langle \mathbf{R}(U), (v - c_\beta)\beta \rangle = \sum_{\beta \in \mathcal{H}} a_\beta \int_{\omega_\beta} r(U)(v - c_\beta)\beta.$$

By Hölder's inequality and the weighted Poincaré-type inequalities given in Theorems 4.1 and 4.3, it follows that

$$\begin{aligned} \langle \mathbf{R}(U), v \rangle &\le \sum_{\beta \in \mathcal{H}} a_\beta \| r(U) \|_{L^2(\omega_\beta, \beta)} \| v - c_\beta \|_{L^2(\omega_\beta, \beta)} \\ &\le C_F \sum_{\beta \in \mathcal{H}} a_\beta \| r(U) \|_{L^2(\omega_\beta, \beta)} \operatorname{diam}(\omega_\beta) \| \nabla v \|_{L^2(\omega_\beta, \beta)} \\ &\le C_F \left(\sum_{\beta \in \mathcal{H}} \| r(U) \|^2_{L^2(\omega_\beta, \beta)} \operatorname{diam}(\omega_\beta)^2 a_\beta \right)^{\frac{1}{2}} \left(\sum_{\beta \in \mathcal{H}} \| \nabla v \|^2_{L^2(\omega_\beta, \beta)} a_\beta \right)^{\frac{1}{2}} \\ &= C_F \left(\sum_{\beta \in \mathcal{H}} \int_{\omega_\beta} |r(U)|^2 \operatorname{diam}(\omega_\beta)^2 a_\beta \beta \right)^{\frac{1}{2}} \| \nabla v \|_{L^2(\Omega)}, \end{aligned}$$

where $C_F > 0$ is the constant satisfying (4.2). In consequence,

$$\| \mathbf{R}(U) \|_{H^{-1}(\Omega)} \le C_F \left(\sum_{\beta \in \mathcal{H}} a_\beta \operatorname{diam}(\omega_\beta)^2 \int_{\omega_\beta} |r(U)|^2 \beta \right)^{\frac{1}{2}}.$$

Regarding (5.1), we finally obtain that

$$\| \nabla (u - U) \|_{L^2(\Omega)} \le \frac{C_F}{\gamma_1} \left(\sum_{\beta \in \mathcal{H}} a_\beta \operatorname{diam}(\omega_\beta)^2 \int_{\omega_\beta} |r(U)|^2 \beta \right)^{\frac{1}{2}}.$$

Let $\{\mathcal{Q}_\ell\}_{\ell \in \mathbb{N}_0}$ be the sequence of underlying Cartesian meshes associated to the different levels as explained in Sec. 3. Without losing generality, we assume that

$$\max_{\ell \in \mathbb{N}_0} \frac{\max_{Q \in \mathcal{Q}_\ell} \operatorname{diam}(Q)}{\min_{Q \in \mathcal{Q}_\ell} \operatorname{diam}(Q)} < \infty,$$

where $\operatorname{diam}(Q)$ denotes the diameter of the cell Q. Now, we define the *meshsize* h_ℓ *at level* ℓ (corresponding to the Cartesian grid $\mathcal{Q}_\ell$) by

$$h_\ell := \max_{Q \in \mathcal{Q}_\ell} \operatorname{diam}(Q), \quad \ell \in \mathbb{N}_0. \tag{5.2}$$

We also define

$$h_\beta := h_\ell, \tag{5.3}$$

where ℓ is such that $\beta \in \mathcal{B}_\ell$; and note that h_β is equivalent to $\operatorname{diam}(\omega_\beta)$.

Finally, for $V \in \operatorname{span}\mathcal{H}$ and $\beta \in \mathcal{H}$, we define the *local error indicator* $\mathcal{E}_{\mathcal{H}}(V,\beta)$ by

$$\mathcal{E}_{\mathcal{H}}(V,\beta) := \sqrt{a_\beta} h_\beta \left(\int_{\omega_\beta} |r(V)|^2 \beta \right)^{\frac{1}{2}}, \tag{5.4}$$

and summarize we have just proved in the following result.

Theorem 5.1. *Let $u \in H_0^1(\Omega)$ be the solution of problem* (2.3) *and $U \in \mathcal{S}_0$ be the Galerkin approximation of u satisfying* (3.6)*. Then, there exists a constant $C_u > 0$ which depends on γ_1 in* (2.2)*, the polynomial degree p and the dimension d, such that*

$$\|\nabla(u-U)\|_{L^2(\Omega)} \le C_u \left(\sum_{\beta \in \mathcal{H}} \mathcal{E}_{\mathcal{H}}(U,\beta)^2 \right)^{\frac{1}{2}}.$$

Remark 5.1. The local error estimators given in (5.4) are associated to each degree of freedom instead of each element as proposed in Ref. 8. Although both kinds of estimators are simple residual-type, we remark that our approach has at least two main advantages. On the one hand, as stated in Theorem 5.1, our function-based estimators are reliable for *arbitrary* hirarchical mesh configurations, whereas the counterpart stated in Theorem 11 in Ref. 8 only holds for certain *admissible* hierarchical meshes (see Definition 4 in Ref. 8) whose implementation requires a recursive refinement strategy. On the other hand, when using local error estimators to guide adaptive procedures, the refinement of single elements may not change the discrete space, whereas the algorithm we propose in Sec. 7 does enrich the space every time and avoids to solve useless linear systems.

Remark 5.2. (On the efficiency of the error estimators) The standard techniques in finite element analysis require some particular inverse estimate in order to prove the so-called *lower bound*.[30] In the context of isogemetric analysis, the constant involved in such an estimate depends on the maximum difference of levels of active cells that there may be within the support of a basis function in $\mathcal{H}$. In other words, such inverse inequality does not hold for arbitrary hierarchical meshes and a rigorous proof of the efficiency of the estimators could be obtained for some kind of admissible meshes. Nevertheless, in practice, we usually obtain bounded efficiency indices without enforcing restrictions on the mesh configurations as illustrated at the end of Sec. 7.

6. Refinement for Hierarchical Spaces and Estimator Reduction

In this section, we explain precisely how to perform the refinement of a hierarchical mesh. In addition, we show that the error estimator defined in the previous section

is reduced after mesh refinement in the sense of Corollary 3.4 in Ref. 9, which is an important property in order to get a proof of linear convergence for adaptive algorithms following the approaches in Refs. 9 and 18 (see Remarks 6.1 and 7.1).

6.1. *Refinement of hierarchical meshes*

We start with the following basic definition.

Definition 6.1. (Enlargement) Let $\mathbf{\Omega}_n := \{\Omega_0, \Omega_1, \dots, \Omega_n\}$ and $\mathbf{\Omega}^*_{n+1} := \{\Omega^*_0, \Omega^*_1, \dots, \Omega^*_n, \Omega^*_{n+1}\}$ be hierarchies of subdomains of Ω of depth (at most) n and $n+1$, respectively. We say that $\mathbf{\Omega}^*_{n+1}$ is an *enlargement* of $\mathbf{\Omega}_n$ if

$$\Omega_\ell \subset \Omega^*_\ell, \quad \ell = 1, 2, \dots, n.$$

In order to enlarge the current subdomains, we have to select the regions in Ω where a more accurate approximation is required. Such a choice can be done by selecting to *refine* some active functions, as we explain in Sec. 7 where we will consider a precise way of enlarging the hierarchy $\mathbf{\Omega}_n$.

If $\mathbf{\Omega}^*_{n+1}$ is an enlargement of $\mathbf{\Omega}_n$, we denote by $\mathcal{H}^*$ the hierarchical basis (associated to the hierarchy $\mathbf{\Omega}^*_{n+1}$) as in Definition 3.2. From Theorem 5.4 in Ref. 7, it follows that

$$\operatorname{span} \mathcal{H} \subset \operatorname{span} \mathcal{H}^*,$$

and thus, we say that $\mathcal{H}^*$ is a *refinement* of $\mathcal{H}$.

Finally, we denote by $\mathcal{Q}^*$ the *refined* hierarchical mesh given by

$$\mathcal{Q}^* := \bigcup_{\ell=0}^{n} \{Q \in \mathcal{Q}_\ell \,|\, Q \subset \Omega^*_\ell \wedge Q \notin \Omega^*_{\ell+1}\}.$$

6.2. *Error estimator reduction*

Let $\{\mathcal{Q}_\ell\}_{\ell \in \mathbb{N}_0}$ be the sequence of underlying Cartesian meshes associated to the different levels as explained in Sec. 3 and let $\{h_\ell\}_{\ell \in \mathbb{N}_0}$ be the sequence of meshsizes defined by (5.2). In order to analyze the behavior of the error estimator under refinement, we assume that the successive levels are obtained performing q-adic refinement in the tensor product meshes. More precisely, we state the following assumption.

Assumption 6.1. There exists $q \in \mathbb{N}$, $q \geq 2$ such that

$$h_{\ell+1} \leq \frac{1}{q} h_\ell, \quad \forall\, \ell \in \mathbb{N}_0.$$

Let $\mathcal{H}$ be the hierarchical basis associated to a hierarchy of subdomains of depth n, $\mathbf{\Omega}_n := \{\Omega_0, \Omega_1, \dots, \Omega_n\}$. Let $\{a_\beta\}_{\beta \in \mathcal{H}}$ be the sequence of positive numbers as in (3.5) such that $\sum_{\beta \in \mathcal{H}} a_\beta \beta(x) = 1$, for $x \in \Omega$. For $V \in \operatorname{span} \mathcal{H}$ and $\beta \in \mathcal{H}$, the local error indicator $\mathcal{E}_{\mathcal{H}}(V, \beta)$ defined in (5.4) is given by

$$\mathcal{E}_{\mathcal{H}}(V, \beta) := \sqrt{a_\beta} h_\beta \left(\int_{\omega_\beta} |r(V)|^2 \beta \right)^{\frac{1}{2}},$$

where h_β is defined by (5.3). Additionally, for $\mathcal{N} \subset \mathcal{H}$, we define $\mathcal{E}_{\mathcal{H}}(V,\mathcal{N})$ by

$$\mathcal{E}_{\mathcal{H}}(V,\mathcal{N}) := \left(\sum_{\beta \in \mathcal{N}} \mathcal{E}^2_{\mathcal{H}}(V,\beta) \right)^{\frac{1}{2}}.$$

We remark that the *global indicator* $\mathcal{E}_{\mathcal{H}}(V,\mathcal{H})$ can be computed as

$$\mathcal{E}_{\mathcal{H}}(V,\mathcal{H}) = \left(\int_\Omega |r(V)|^2 H^2_{\mathcal{H}} \right)^{\frac{1}{2}} = \|r(V)\|_{L^2(\Omega, H^2_{\mathcal{H}})},$$

where the function $H^2_{\mathcal{H}} \in \operatorname{span} \mathcal{H}$ is given by

$$H^2_{\mathcal{H}} := \sum_{\beta \in \mathcal{H}} a_\beta h^2_\beta \beta. \tag{6.1}$$

The main result of this section is the following proposition.

Proposition 6.1. (*Estimator reduction*) *Let* $\{h_\ell\}_{\ell \in \mathbb{N}_0}$ *be the meshsizes defined in* (5.2) *and let Assumption* 6.1 *be valid. Let* $\mathcal{H}$ *be a hierarchical basis and let* $\mathcal{H}^*$ *be a refinement of* $\mathcal{H}$*. If* $\mathcal{R} := \mathcal{H} \setminus \mathcal{H}^*$ *denotes the set of* refined basis functions, *then*

$$\mathcal{E}^2_{\mathcal{H}^*}(V,\mathcal{H}^*) \leq \mathcal{E}^2_{\mathcal{H}}(V,\mathcal{H}) - \lambda \mathcal{E}^2_{\mathcal{H}}(V,\mathcal{R}), \quad \forall\, V \in \operatorname{span} \mathcal{H},$$

where $\lambda := \left(1 - \frac{1}{q^2}\right)$.

This result is a consequence of Lemma 6.2. In the proof of that lemma, we will use the following result which is a consequence of the fact that deactivated functions of level ℓ (in $\mathcal{H}^*$) can be written in terms of active functions of higher levels (in $\mathcal{H}^*$). More precisely, from Lemma 5.4 in Ref. 7, we have that

$$\{\beta_\ell \in \mathcal{B}_\ell \mid \operatorname{supp} \beta_\ell \subset \Omega^*_{\ell+1}\} \subset \operatorname{span}\left(\mathcal{H}^* \cap \bigcup_{k=\ell+1}^{n} \mathcal{B}_k \right), \quad \ell = 0, 1, \ldots, n-1. \tag{6.2}$$

Lemma 6.1. *Let* $\mathcal{H}$ *be a hierarchical basis and let* $\mathcal{H}^*$ *be a refinement of* $\mathcal{H}$*. If* $\mathcal{R} := \mathcal{H} \setminus \mathcal{H}^*$ *denotes the set of refined functions, then*

$$\mathcal{R}_\ell := \mathcal{R} \cap \mathcal{B}_\ell \subset \operatorname{span}\left(\mathcal{H}^* \cap \bigcup_{k=\ell+1}^{n} \mathcal{B}_k \right), \quad \ell = 0, 1, \ldots, n-1.$$

Proof. Let $\beta_\ell \in \mathcal{R}_\ell$ for some $\ell = 0, 1, \ldots, n-1$. Since $\beta_\ell \in \mathcal{H} \cap \mathcal{B}_\ell$, $\operatorname{supp} \beta_\ell \subset \Omega_\ell \subset \Omega^*_\ell$. Thus, we have that $\operatorname{supp} \beta_\ell \subset \Omega^*_{\ell+1}$ due to $\beta_\ell \notin \mathcal{H}^*$. Finally, (6.2) implies that $\beta_\ell \in \operatorname{span}(\mathcal{H}^* \cap \bigcup_{k=\ell+1}^{n} \mathcal{B}_k)$. □

Lemma 6.2. *Let* $\{h_\ell\}_{\ell \in \mathbb{N}_0}$ *be the meshsizes defined in* (5.2) *and let Assumption* 6.1 *be valid. Let* $\mathcal{H}$ *be a hierarchical basis and let* $\mathcal{H}^*$ *be a refinement of* $\mathcal{H}$*. If* $\mathcal{R} := \mathcal{H} \setminus \mathcal{H}^*$ *denotes the set of refined functions, then*

$$H^2_{\mathcal{H}^*}(x) \leq H^2_{\mathcal{H}}(x) - \left(1 - \frac{1}{q^2}\right) \sum_{\beta \in \mathcal{R}} a_\beta h^2_\beta \beta(x), \quad \forall\, x \in \Omega,$$

where $H_{\mathcal{H}}$ *and* $H_{\mathcal{H}^*}$ *are defined as in* (6.1)*, and* $q \geq 2$ *is the constant appearing in Assumption* 6.1.

Proof. Note that

$$1 = \sum_{\beta \in \mathcal{H}} a_\beta \beta(x) = \sum_{\beta \in \mathcal{H} \setminus \mathcal{R}} a_\beta \beta(x) + \sum_{\ell=0}^{n-1} \sum_{\beta \in \mathcal{R}_\ell} a_\beta \beta(x), \quad \forall\, x \in \Omega.$$

By Lemma 6.1, we have that $\beta_\ell := \sum_{\beta \in \mathcal{R}_\ell} a_\beta \beta \in \operatorname{span}(\mathcal{H}^* \cap \bigcup_{k=\ell+1}^n \mathcal{B}_k)$ and therefore,

$$\beta_\ell = \sum_{\beta \in \mathcal{H}^* \cap \bigcup_{k=\ell+1}^n \mathcal{B}_k} c_{\beta,\ell} \beta,$$

for some constants $c_{\beta,\ell}$. Then,

$$\sum_{\beta \in \mathcal{H} \setminus \mathcal{R}} a_\beta \beta(x) + \sum_{\ell=0}^{n-1} \sum_{\beta \in \mathcal{H}^* \cap \bigcup_{k=\ell+1}^n \mathcal{B}_k} c_{\beta,\ell} \beta(x) = 1, \quad \forall\, x \in \Omega. \tag{6.3}$$

Note that the last equation gives a partition of unity with functions $\mathcal{H}^*$. Let $\{a^*_\beta\}_{\beta \in \mathcal{H}^*}$ be the sequence of positive numbers such that

$$\sum_{\beta \in \mathcal{H}^*} a^*_\beta \beta(x) = 1, \quad \forall\, x \in \Omega. \tag{6.4}$$

Note that the difference between (6.3) and (6.4) is that in the former, some basis functions appear more than once. Finally, taking into account Assumption 6.1, we have that

$$\begin{aligned} H^2_{\mathcal{H}^*} &= \sum_{\beta \in \mathcal{H}^*} a^*_\beta h^2_\beta \beta = \sum_{\beta \in \mathcal{H}[\setminus]\mathcal{R}} a_\beta h^2_\beta \beta + \sum_{\ell=0}^{n-1} \sum_{\beta \in \mathcal{H}^* \cap \bigcup_{k=\ell+1}^n \mathcal{B}_k} h^2_\beta c_{\beta,\ell} \beta \\ &\le \sum_{\beta \in \mathcal{H} \setminus \mathcal{R}} a_\beta h^2_\beta \beta + \sum_{\ell=0}^{n-1} h^2_{\ell+1} \beta_\ell \\ &\le \sum_{\beta \in \mathcal{H} \setminus \mathcal{R}} a_\beta h^2_\beta \beta + \frac{1}{q^2} \sum_{\ell=0}^{n-1} h^2_\ell \beta_\ell = \sum_{\beta \in \mathcal{H} \setminus \mathcal{R}} a_\beta h^2_\beta \beta + \frac{1}{q^2} \sum_{\beta \in \mathcal{R}} a_\beta h^2_\beta \beta \\ &= H^2_{\mathcal{H}} - \left(1 - \frac{1}{q^2}\right) \sum_{\beta \in \mathcal{R}} a_\beta h^2_\beta \beta, \end{aligned}$$

which concludes the proof. □

We finish this section with the proof of the estimator reduction property.

Proof of Proposition 6.1. Let $V \in \operatorname{span} \mathcal{H}$ and let $\lambda := (1 - \frac{1}{q^2})$. By Lemma 6.2, we have that

$$\begin{aligned} \mathcal{E}^2_{\mathcal{H}^*}(V, \mathcal{H}^*) &= \int_\Omega |r(V)|^2 H^2_{\mathcal{H}^*} \le \int_\Omega |r(V)|^2 \left(H^2_{\mathcal{H}} - \lambda \sum_{\beta \in \mathcal{R}} a_\beta h^2_\beta \beta \right) \\ &= \int_\Omega |r(V)|^2 H^2_{\mathcal{H}} - \lambda \sum_{\beta \in \mathcal{R}} \int_\Omega |r(V)|^2 a_\beta h^2_\beta \beta \end{aligned}$$

$$= \mathcal{E}^2_{\mathcal{H}}(V,\mathcal{H}) - \lambda \sum_{\beta\in\mathcal{R}} \mathcal{E}^2_{\mathcal{H}}(V,\beta)$$

$$= \mathcal{E}^2_{\mathcal{H}}(V,\mathcal{H}) - \lambda \mathcal{E}^2_{\mathcal{H}}(V,\mathcal{R}). \qquad \square$$

Remark 6.1. (Estimator reduction property) Let $U \in \mathcal{S}_0 = \mathcal{S}_0(\mathcal{Q})$ and $U^* \in \mathcal{S}_0^* := \mathcal{S}_0(\mathcal{Q}^*)$ denote the Galerkin solutions of the discrete problem (3.6) on the spaces $\operatorname{span}\mathcal{H}$ and $\operatorname{span}\mathcal{H}^*$, respectively. Let $\mathcal{R} := \mathcal{H} \setminus \mathcal{H}^*$. In view of Proposition 6.1, it can be proved that there exists a constant $C_E > 0$ such that

$$\mathcal{E}^2_{\mathcal{H}^*}(U^*,\mathcal{H}^*) \le (1+\delta)(\mathcal{E}^2_{\mathcal{H}}(U,\mathcal{H}) - \lambda\mathcal{E}^2_{\mathcal{H}}(U,\mathcal{R})) + (1+\delta^{-1})C_E \|\nabla(U^* - U)\|, \quad (6.5)$$

for all $\delta > 0$, provided the following *inverse inequality* holds:

$$\|\Delta V\|_{L^2(\Omega,H^2_{\mathcal{H}})} \le C\|\nabla V\|_{L^2(\Omega)}, \quad \forall\, V \in \operatorname{span}\mathcal{H} \quad (6.6)$$

with a constant $C > 0$ independent of $\mathcal{H}$. As already pointed out in Remark 5.2, an inverse estimate like (6.6) does not hold for arbitrary hierarchical mesh configurations. However, if for each $\beta \in \mathcal{H}$, the elements in the hierarchical mesh $\mathcal{Q}$ which are within its support belong to at most a fixed number of different levels, (6.6) can be proved using standard arguments due to $H_{\mathcal{H}|_Q}$ is equivalent to the local mesh size $\operatorname{diam}(Q)$ in this kind of meshes.

7. Adaptive Loop and Numerical Examples

In this section, we propose an adaptive algorithm guided by the *a posteriori* error estimators defined in Sec. 5. Additionally, we show the performance of such an adaptive procedure in practice through several numerical examples.

The adaptive loop that we consider is quite standard and consists of the following modules:

$$\text{SOLVE} \to \text{ESTIMATE} \to \text{MARK} \to \text{REFINE}. \quad (7.1)$$

We start with a tensor product mesh and the corresponding spline space, regarded as the current hierarchical mesh $\mathcal{Q}$ and hierarchical space $\mathcal{S}(\mathcal{Q}) = \operatorname{span}\mathcal{H}$, respectively. We perform the steps in (7.1) in order to get an adaptively refined mesh $\mathcal{Q}^*$ and its corresponding hierarchical space $\mathcal{S}(\mathcal{Q}^*) = \operatorname{span}\mathcal{H}^*$. Next, we consider $\mathcal{Q}^*$ and $\mathcal{H}^*$ as the current hierarchical mesh and basis, respectively, and perform the steps in (7.1), and so on. We now briefly describe the modules of the adaptive loop:

- SOLVE: Compute the solution U of the discrete problem (3.6) in the current hierarchical space $\mathcal{S}(\mathcal{Q}) = \operatorname{span}\mathcal{H}$.
- ESTIMATE: Use the current discrete solution U to compute the *a posteriori error estimators* $\mathcal{E}_\beta := \mathcal{E}_{\mathcal{H}}(U,\beta)$ defined in (5.4), for each $\beta \in \mathcal{H}$.
- MARK: Use the *a posteriori* error estimators $\{\mathcal{E}_\beta\}_{\beta\in\mathcal{H}}$ to compute the set of *marked functions* $\mathcal{M} \subset \mathcal{H}$ using some marking strategy.

- REFINE: Use the set of marked functions $\mathcal{M}$ to enlarge the current hierarchy of subdomains $\mathbf{\Omega}_n := \{\Omega_0, \Omega_1, \ldots, \Omega_n\}$ as follows:

  Let $\mathcal{M}_\ell := \mathcal{M} \cap \mathcal{B}_\ell$, for $\ell = 0, 1, \ldots, n-1$. Now, we define the hierarchy of subdomains $\mathbf{\Omega}^*_{n+1} := \{\Omega^*_0, \Omega^*_1, \ldots, \Omega^*_n, \Omega^*_{n+1}\}$ of depth at most $n+1$, by

$$\begin{cases} \Omega^*_0 := \Omega_0, \\ \Omega^*_\ell := \Omega_\ell \cup \bigcup_{\beta \in \mathcal{M}_{\ell-1}} \operatorname{supp} \beta, \quad \ell = 1, 2, \ldots, n, \\ \Omega^*_{n+1} := \varnothing. \end{cases} \tag{7.2}$$

  If $\mathcal{H}^*$ is the hierarchical basis associated to $\mathbf{\Omega}^*_{n+1}$, we note that $\mathcal{M} \subset \mathcal{H} \setminus \mathcal{H}^*$; in other words, at least the functions in $\mathcal{M}$ have been refined and removed from the hierarchical basis $\mathcal{H}$.

Remark 7.1. (Linear convergence) It is possible to prove a contraction property for the proposed algorithm following the lines of the proof of Theorem 4.1 in Ref. 9 when the bilinear form B is symmetric or Theorem 4.1 in Ref. 18 in the general non-symmetric case. More precisely, it needed only the following main ingredients:

- A *quasi-orthogonality property* (see for instance, Proposition 3.6 in Ref. 18).
- Given a user parameter $\theta \in (0, 1)$, mark according to *Dörfler's criterion*, which consists in selecting a set $\mathcal{M} \subset \mathcal{H}$ such that

$$\sum_{\beta \in \mathcal{M}} \mathcal{E}^2_\beta \geq \theta \sum_{\beta \in \mathcal{H}} \mathcal{E}^2_\beta. \tag{7.3}$$

- An *estimator reduction property* as given in (6.5).
- A *global upper bound* as given by Theorem 5.1.

Remark 7.2. (Complexity of the module REFINE) Unlike what happens for standard finite elements,[5,35] we can bound the number of degrees of freedom (DOFs) $\#\mathcal{H}^*$ after refining the basis $\mathcal{H}$ in terms of the number marked basis functions $\#\mathcal{M}$. More precisely, we have that

$$\#\mathcal{H}^* - \#\mathcal{H} \leq C \#\mathcal{M},$$

where the constant $C > 0$ is independent of $\mathcal{H}, \mathcal{H}^*$ and $\mathcal{M}$. Indeed, the constant C depends on the following:

- The maximum number of neighbors of a B-spline β in the tensor product basis $\mathcal{B}_\ell$, that is, those B-splines' supports share at least one cell with the support of β (cf. Ref. 20). This bound is independent of the level ℓ and only depends on the polynomial degrees $\mathbf{p} = (p_1, p_2, \ldots, p_d)$.
- The maximum number of children of a B-spline $\beta \in \mathcal{B}_\ell$. This bound can also be taken independent of the level ℓ, and if the subsequent levels in (3.3) are obtained by dyadic refinement, such a bound depends solely on the polynomial degrees $\mathbf{p} = (p_1, p_2, \ldots, p_d)$.

Now, we present some numerical tests to show the performance of the proposed algorithm. In the module MARK, we use the *maximum strategy* with parameter $\theta = 0.5$, that is, $\mathcal{M} \subset \mathcal{H}$ consists of the basis functions $\beta \in \mathcal{H}$ such that

$$\mathcal{E}_\beta \geq \theta \max_{\beta' \in \mathcal{H}} \mathcal{E}_{\beta'}.$$

We prefer to exhibit the numerical tests using the maximum strategy instead Dörfler criterion (7.3) just to show that the algorithm also performs well. The implementation of the adaptive procedure was done using the data structure and algorithms introduced in Ref. 20. In particular, we study the decay of the energy error in terms of DOFs in each example, and analyze the rates of convergence.

We consider the problem

$$\begin{cases} -\Delta u = f & \text{in } \Omega, \\ u = g & \text{on } \partial\Omega, \end{cases} \tag{7.4}$$

giving in each particular example the definition of the domain Ω and the problem data f and g.

Example 7.1. (Regular solution in the unit square) We consider $\Omega = [0,1] \times [0,1]$ and the problem data f and g in (7.4) are chosen such that the exact solution u is given by $u(x,y) = e^{-100((x-\frac{1}{2})^2+(y-\frac{1}{2})^2)}$. In Fig. 1, we plot the exact solution, some hierarchical meshes and the decay of the relative energy error versus DOFs for

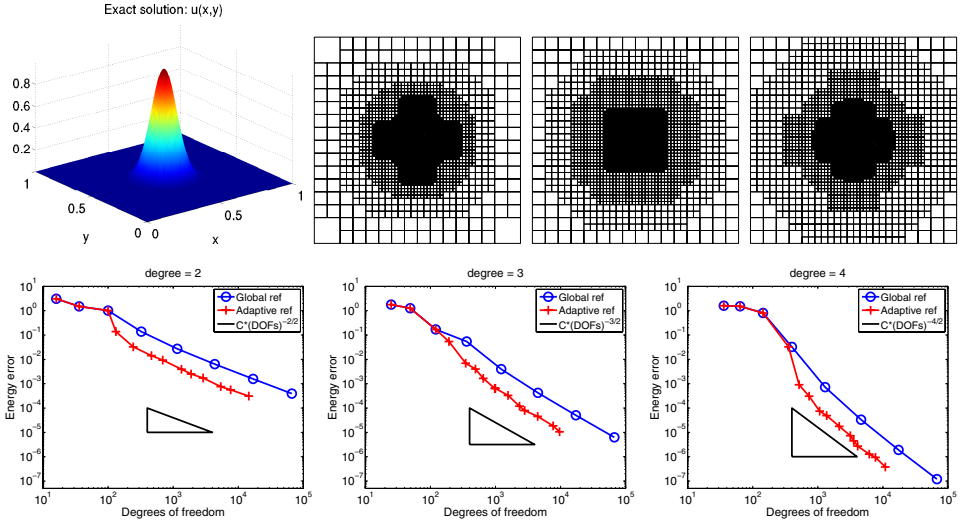

Fig. 1. Some hierarchical meshes for the solution of Example 7.1; for biquadratics with 3064 elements and 2884 DOFs (top left), bicubics with 3028 elements and 2809 DOFs (top middle) and biquartics with 3400 elements and 3160 DOFs (top right). Note that although all meshes have nearly the same amount of elements, the refinement is more spread for high order splines due to the sizes of the basis function supports. We plot the relative energy error $|u-U|_{H^1(\Omega)}/|u|_{H^1(\Omega)}$ versus DOFs; for biquadratics (bottom left), bicubics (bottom middle) and biquartics (bottom right).

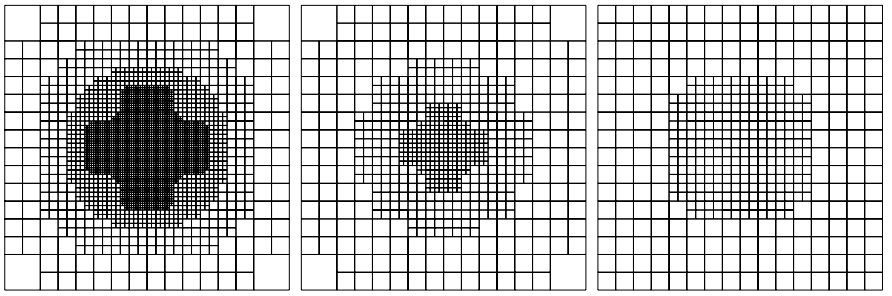

Fig. 2. Comparison of adaptive meshes obtained for Example 7.1 using different polynomial degrees, obtaining in all cases that $|u - U|_{H^1(\Omega)}/|u|_{H^1(\Omega)} \approx 10^{-3}$. The mesh for biquadratics has 3064 elements and 2884 DOFs (left), the mesh bicubics has 688 elements and 649 DOFs (middle) and the mesh for biquartics has 436 elements and 516 DOFs (right).

different spline degrees. As expected, both tensor product meshes and hierarchical meshes reach optimal orders of convergence, but note that in all cases, the curves corresponding to the adaptive strategy are quite below the others. For example, for attaining an relative error of around $1.7 \cdot 10^{-4}$ using biquadratics, the global refinement requires 66,564 DOFs whereas the adaptive strategy only needs 14,548 DOFs.

Additionally, in Fig. 2, we present the adaptive meshes obtained for different polynomial degrees, starting with an initial tensor product mesh of four elements, reaching in all cases an relative energy error $\approx 10^{-3}$. It is interesting to remark that although it is well known[3] that the element-by-element assembly is very costly for higher degree, the use of adaptivity changes this picture. Indeed, due to the reduced number of elements for bicubics and biquartics, the time-to-solution for bicubics is 35% and for biquartics is 17% of the time-to-solution for biquadratics.

Example 7.2. (Diagonal refinement in the unit square) We take $\Omega = [0,1] \times [0,1]$ and choose f and g such that the exact solution u of (7.4) is given by $u(x,y) = \tan^{-1}(25(x-y))$. In Fig. 3, we plot the exact solution, some hierarchical meshes and the decay of the relative energy error versus DOFs for different spline degrees. As in the previous example, both tensor product meshes and hierarchical meshes reach optimal orders of convergence, but note that in all cases, the curves corresponding to the adaptive strategy are again significantly lower than the others. For example, for attaining a relative energy error of around 10^{-6} using biquadratics, the global refinement requires 67,600 DOFs whereas the adaptive strategy only needs 10,186 DOFs.

Example 7.3. (Singular domain: An L-shaped domain) We consider the L-shaped domain $\Omega = [-1,1]^2 \setminus ((0,1) \times (-1,0))$ and choose f and g such that the exact solution u of (7.4) is given in polar coordinates by $u(\rho,\varphi) = \rho^{2/3}\sin(2\varphi/3)$. In Fig. 4, we plot the exact solution, some hierarchical meshes and the decay of the relative energy error versus DOFs for different spline degrees. We note that the

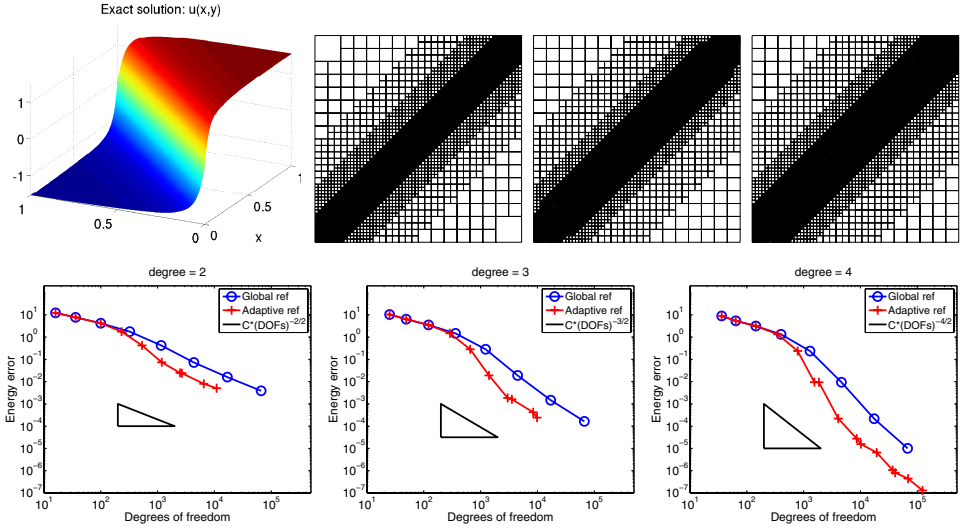

Fig. 3. Some hierarchical meshes for the solution of Example 7.2; for biquadratics with 11,578 elements and 10,958 DOFs (top left), bicubics with 10,792 elements and 9865 DOFs (top middle) and biquartics with 11,338 elements and 10,186 DOFs (top right). Note that although all meshes have nearly the same amount of elements, the refinement is more spread for high order splines due to the sizes of the basis function supports. We plot the relative energy error $|u-U|_{H^1(\Omega)}/|u|_{H^1(\Omega)}$ versus DOFs; for biquadratics (bottom left), bicubics (bottom middle) and biquartics (bottom right).

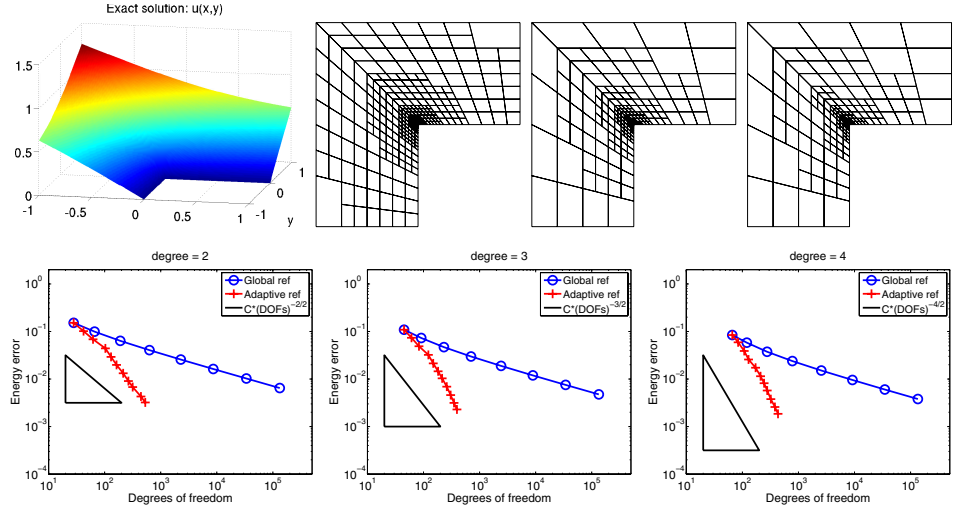

Fig. 4. Some hierarchical meshes for the solution of Example 7.3 obtaining in all cases $|u-U|_{H^1(\Omega)}/|u|_{H^1(\Omega)} \approx 2\cdot 10^{-3}$; for biquadratics with 500 elements and 530 DOFs (top left), bicubics with 314 elements and 350 DOFs (top middle) and biquartics with 254 elements and 322 DOFs (top right). In addition, we plot the relative energy error $|u-U|_{H^1(\Omega)}/|u|_{H^1(\Omega)}$ versus DOFs; for biquadratics (bottom left), bicubics (bottom middle) and biquartics (bottom right).

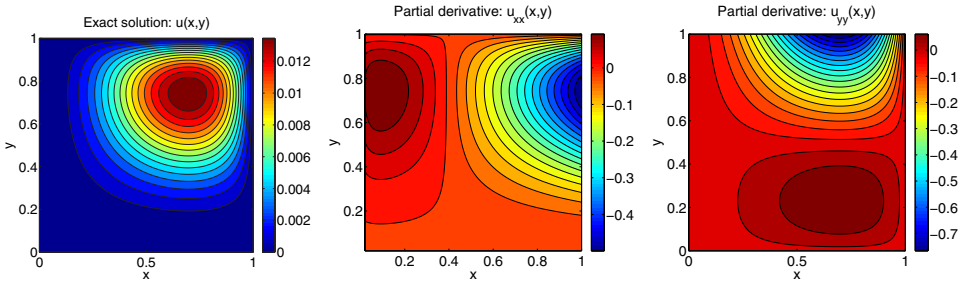

Fig. 5. The exact solution $u(x,y) = x^{2.3}(1-x)y^{2.9}(1-y)$ (left) corresponding to Example 7.4 and its derivatives u_{xx} (middle) and u_{yy} (right).

global refinement associated to tensor product spaces does not reach the optimal order of convergence due to the singularity. In contrast to this, the adaptive strategy seems to recover the optimal decay for the energy error given by $\mathcal{O}((\#\text{DOFs})^{\frac{p}{2}})$, although in the curves of Fig. 4, a faster preasymptotic behavior is observed which is very useful for practical purposes.

Example 7.4. (Singular solution in the unit square) We consider a problem whose solution is not too smooth. Specifically, we take $\Omega = [0,1] \times [0,1]$, and choose $g \equiv 0$ and f such that the exact solution u of (7.4) is given by $u(x,y) = x^{2.3}(1-x)y^{2.9}(1-y)$. Note that in this case, $u \in H^2(\Omega) \setminus H^3(\Omega)$ and there are singularities along the sides $x = 0$ and $y = 0$, being a bit stronger than the singularity along $x = 0$; see Fig. 5. Some hierarchical meshes and the error decay in terms of DOFs for different polynomial degrees are presented in Fig. 6. We note that both global refinement and the adaptive refinement reach the optimal order of convergence when using biquadratics (bottom left), but only the adaptive refinement converges with optimal rates when using bicubics (bottom middle) and biquartics (bottom right), due to the singularity of the solution.

Example 7.5. (A physical domain: A quarter of ring) In this case, we consider the domain Ω given in polar coordinates by $\Omega = \{(\rho,\varphi) \,|\, 1 \le \rho \le 2 \wedge 0 \le \varphi \le \frac{\pi}{2}\}$ and we choose the problem data f and g in (7.4) such that the exact solution u is given by $u(x,y) = e^{-100((x-\frac{1}{2})^2+(y-\frac{1}{2})^2)}$. Despite the optimal rates of convergence which are reached by using both tensor product meshes and hierarchical meshes (see Fig. 7), we emphasize that in this case, the adaptive strategy is still convenient. As an example, we note that to get a relative energy error of $5 \cdot 10^{-5}$ using bicubics, the adaptive strategy requires less than 3% of the DOFs utilized by the global refinement, because the former procedure requires 1900 DOFs whereas the latter needs 67,081 DOFs.

Example 7.6. (A 3*d*-domain: The unit cube) We consider the cube $\Omega = [0,1]^3$ and choose f and g such that the exact solution u of (7.4) is given by $u(x,y,z) = e^{-100((x-\frac{1}{2})^2+(y-\frac{1}{2})^2+(z-\frac{1}{2})^2)}$. Since the solution is smooth enough, both strategies

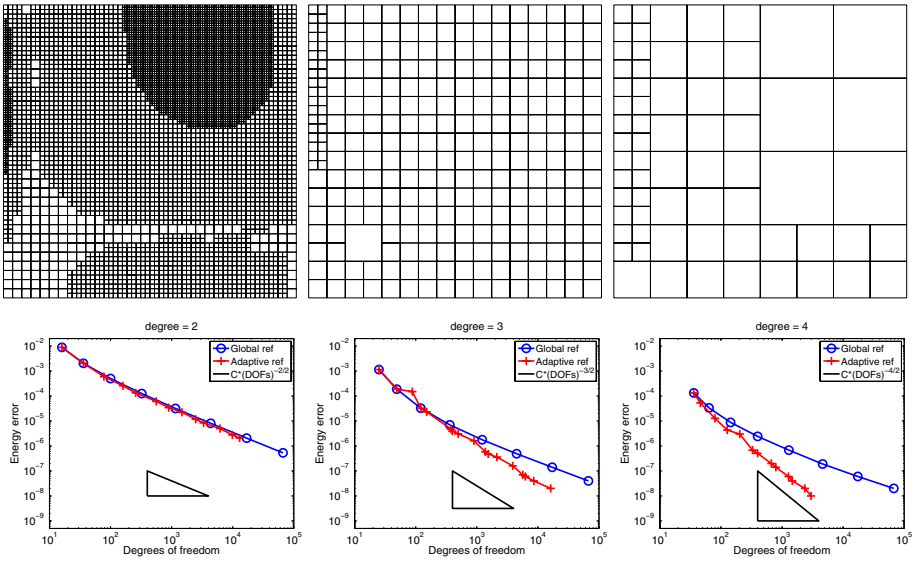

Fig. 6. Comparison of adaptive meshes for the solution of Example 7.4 for different polynomial degrees, obtaining in all cases, $|u-U|_{H^1(\Omega)}/|u|_{H^1(\Omega)} \approx 1.5 \cdot 10^{-4}$. The mesh for biquadratics has 6139 elements and 6213 DOFs (top left), the mesh for bicubics has 280 elements and 379 DOFs (top middle) and the mesh for biquartics has 67 elements and 127 DOFs (top right). On the other hand, we plot the relative energy error $|u-U|_{H^1(\Omega)}/|u|_{H^1(\Omega)}$ versus DOFs for different polynomial degrees.

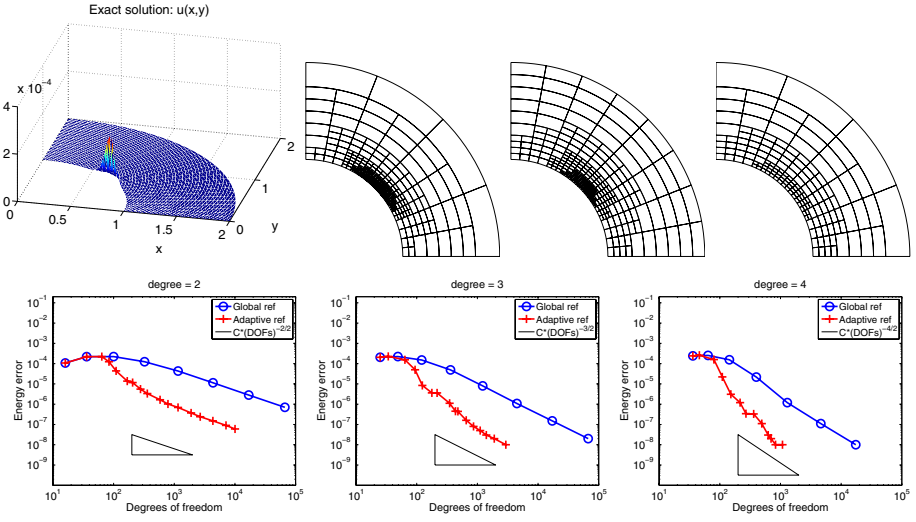

Fig. 7. Some hierarchical meshes for the solution of Example 7.5 obtaining $|u-U|_{H^1(\Omega)}/|u|_{H^1(\Omega)} \approx 2.5 \cdot 10^{-3}$ in all cases; for biquadratics with 802 elements and 788 DOFs (top left), bicubics with 316 elements and 349 DOFs (top middle) and biquartics with 160 elements and 216 DOFs (top right). We plot the relative energy error $|u-U|_{H^1(\Omega)}/|u|_{H^1(\Omega)}$ versus DOFs; for biquadratics (bottom left), bicubics (bottom middle) and biquartics (bottom right).

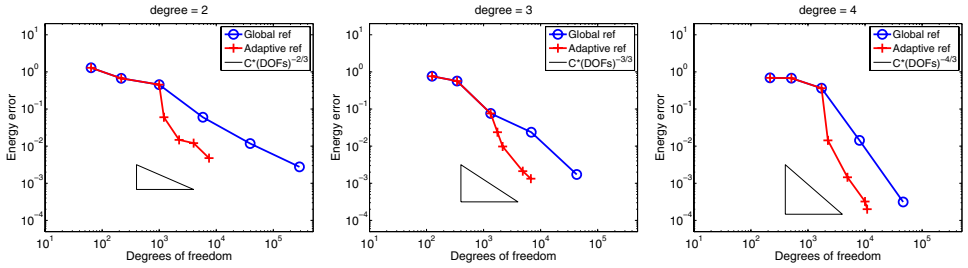

Fig. 8. Energy error decay in terms of DOFs for the solution of the Example 7.6; using biquadratics (left), bicubics (middle) and biquartics (right).

reach optimal orders of convergence, as shown in Fig. 8. However, we note that in all cases, the curves corresponding to the adaptive strategy are the lowest ones, which in practice is equivalent to achieve a given accuracy with considerably fewer DOFs.

7.1. *On the efficiency of the error estimators*

Finally, we analyze the behavior of the efficiency index $\frac{(\sum_{\beta\in\mathcal{H}}\mathcal{E}_\beta^2)^{\frac{1}{2}}}{\|\nabla(u-U)\|_{L^2(\Omega)}}$. In Fig. 9, we plot this index at each iteration step for all the examples previously presented. We see that the energy error $\|\nabla(u-U)\|_{L^2(\Omega)}$ and the global *a posteriori* error estimator $(\sum_{\beta\in\mathcal{H}}\mathcal{E}_\beta^2)^{\frac{1}{2}}$ are equivalent quantities, that is, there exists constants c_1 and c_2 such

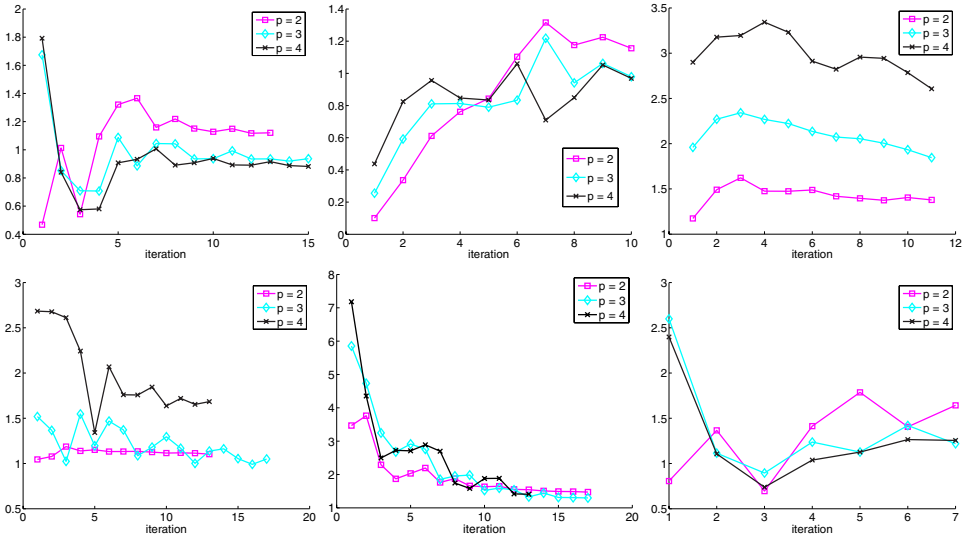

Fig. 9. Efficiency indices $\frac{(\sum_{\beta\in\mathcal{H}}\mathcal{E}_\beta^2)^{\frac{1}{2}}}{\|\nabla(u-U)\|_{L^2(\Omega)}}$; for Example 7.1 (top left), Example 7.2 (top middle), Example 7.3 (top right), Example 7.4 (bottom left), Example 7.5 (bottom middle), Example 7.6 (bottom right).

that

$$0 < c_1 \leq \frac{(\sum_{\beta \epsilon \mathcal{H}} \mathcal{E}_\beta^2)^{\frac{1}{2}}}{\|\nabla(u-U)\|_{L^2(\Omega)}} \leq c_2,$$

at each iteration step. Thus, we conclude that our estimators are not only reliable in the sense of Theorem 5.1 but also experimentally efficient.

Acknowledgments

A. Buffa was partially supported by ERC AdG project CHANGE n. 694515, by MIUR PRIN project "Metodologie innovative nella modellistica differenziale numerica", and by Istituto Nazionale di Alta Matematica (INdAM). E. M. Garau was partially supported by CONICET through Grant PIP 112-2015-0100661, by Universidad Nacional del Litoral through Grants CAI+D 500 201101 00029 LI, 501 201101 00476 LI, 504 201501 00022 LI, by Agencia Nacional de Promoción Científica y Tecnológica, through Grants PICT-2012-2590 and PICT-2014-2522 (Argentina). This support is gratefully acknowledged.

References

1. M. Ainsworth and J. T. Oden, *A Posteriori Error Estimation in Finite Element Analysis* (John Wiley & Sons, 2000).
2. C. Anitescu, M. N. Hossain and T. Rabczuk, Recovery-based error estimation and adaptivity using high-order splines over hierarchical T-meshes, *Comput. Methods Appl. Mech. Engrg.* **328** (2018) 638–662.
3. P. Antolin, A. Buffa, F. Calabrò, M. Martinelli and G. Sangalli, Efficient matrix computation for tensor-product isogeometric analysis: The use of sum factorization, *Comput. Methods Appl. Mech. Engrg.* **285** (2015) 817–828.
4. L. Beirão da Veiga, A. Buffa, G. Sangalli and R. Vázquez, Analysis-suitable T-splines of arbitrary degree: Definition, linear independence and approximation properties, *Math. Models Methods Appl. Sci.* **23** (2013) 1979–2003.
5. P. Binev, W. Dahmen and R. DeVore, Adaptive finite element methods with convergence rates, *Numer. Math.* **97** (2004) 219–268.
6. A. Bressan, Some properties of LR-splines, *Comput. Aided Geom. Design.* **30** (2013) 778–794.
7. A. Buffa and E. M. Garau, Refinable spaces and local approximation estimates for hierarchical splines, *IMA J. Numer. Anal.* **37** (2016) 1125–1149.
8. A. Buffa and C. Giannelli, Adaptive isogeometric methods with hierarchical splines: Error estimator and convergence, *Math. Models Methods Appl. Sci.* **26** (2016) 1–25.
9. J. M. Cascon, C. Kreuzer, R. H. Nochetto and K. G. Siebert, Quasi-optimal convergence rate for an adaptive finite element method, *SIAM J. Numer. Anal.* **46** (2008) 2524–2550.
10. S.-K. Chua and R. L. Wheeden, Estimates of best constants for weighted Poincaré inequalities on convex domains, *Proc. London Math. Soc.* **93** (2006) 197–226.
11. J. A. Cottrell, T. J. R. Hughes and Y. Bazilevs, *Isogeometric Analysis*: *Toward Integration of CAD and FEA* (John Wiley & Sons, 2009).
12. H. B. Curry and I. J. Schoenberg, On Pólya frequency functions. IV. The fundamental spline functions and their limits, *J. Anal. Math.* **17** (1966) 71–107.

13. C. de Boor, *A Practical Guide to Splines*, *Volume 27 of Applied Mathematical Sciences*, revised edn. (Springer-Verlag, 2001).
14. T. Dokken, T. Lyche and K. F. Pettersen, Polynomial splines over locally refined box-partitions, *Comput. Aided Geom. Design* **30** (2013) 331–356.
15. M. Dörfel, B. Jüttler and B. Simeon, Adaptive isogeometric analysis by local *h*-refinement with T-splines, *Comput. Methods Appl. Mech. Engrg.* **199** (2010) 264–275.
16. M. Feischl, G. Gantner, A. Haberl and D. Praetorius, Optimal convergence for adaptive IGA boundary element methods for weakly-singular integral equations, *Numer. Math.* **136** (2017) 147–182.
17. M. Feischl, G. Gantner and D. Praetorius, Reliable and efficient *a posteriori* error estimation for adaptive IGA boundary element methods for weakly-singular integral equations, *Comput. Methods Appl. Mech. Engrg.* **290** (2015) 362–386.
18. M. Feischl, T. Führer and D. Praetorius, Adaptive FEM with optimal convergence rates for a certain class of nonsymmetric and possibly nonlinear problems, *SIAM J. Numer. Anal.* **52** (2014) 601–625.
19. G. Gantner, D. Haberlik and D. Praetorius, Adaptive IGAFEM with optimal convergence rates: Hierarchical B-splines, *Math. Models Methods Appl. Sci.* **27** (2017) 2631–2674.
20. E. M. Garau and R. Vázquez, Algorithms for the implementation of adaptive isogeometric methods using hierarchical B-splines, *Appl. Numer. Math.* **123** (2018) 58–87.
21. C. Giannelli, B. Jüttler and H. Speleers, THB-splines: The truncated basis for hierarchical splines, *Comput. Aided Geom. Design.* **29** (2012) 485–498.
22. C. Giannelli, B. Jüttler and H. Speleers, Strongly stable bases for adaptively refined multilevel spline spaces, *Adv. Comput. Math.* **40** (2014) 459–490.
23. T. J. R. Hughes, J. A. Cottrell and Y. Bazilevs, Isogeometric analysis: CAD, finite elements, NURBS, exact geometry and mesh refinement, *Comput. Methods Appl. Mech. Eng.* **194** (2005) 4135–4195.
24. K. A. Johannessen, T. Kvamsdal and T. Dokken, Isogeometric analysis using LR B-splines, *Comput. Methods Appl. Mech. Eng.* **269** (2014) 471–514.
25. S. K. Kleiss and S. K. Tomar, Guaranteed and sharp *a posteriori* error estimates in isogeometric analysis, *Comput. Math. Appl.* **70** (2015) 167–190.
26. R. Kraft, Adaptive and linearly independent multilevel *B*-splines, in *Surface Fitting and Multiresolution Methods* (*Chamonix–Mont-Blanc*, *1996*) (Vanderbilt Univ. Press, 1997), pp. 209–218.
27. M. Kumar, T. Kvamsdal and K. A. Johannessen, Simple *a posteriori* error estimators in adaptive isogeometric analysis, *Comput. Math. Appl.* **70** (2015) 1555–1582.
28. M. Kumar, T. Kvamsdal and K. A. Johannessen, Superconvergent patch recovery and *a posteriori* error estimation technique in adaptive isogeometric analysis, *Comput. Methods Appl. Mech. Eng.* **316** (2017) 1086–1156.
29. P. Morin, R. H. Nochetto and K. G. Siebert, Local problems on stars: *A posteriori* error estimators, convergence, and performance, *Math. Comp.* **72** (2003) 1067–1097.
30. R. H. Nochetto and A. Veeser, Primer of adaptive finite element methods, in *Multiscale and Adaptivity: Modeling, Numerics and Applications*, Lecture Notes in Mathematics, Vol. 2040 (Springer, 2012), pp. 125–225.
31. L. L. Schumaker, *Spline Functions: Basic Theory*, 3rd edn. (Cambridge Univ. Press, 2007).
32. M. A. Scott, X. Li, T. W. Sederberg and T. J. R. Hughes, Local refinement of analysis-suitable T-splines, *Comput. Methods Appl. Mech. Eng.* **213** (2012) 206–222.
33. H. Speleers and C. Manni, Effortless quasi-interpolation in hierarchical spaces, *Numer. Math.* (2015), pp. 1–30.

34. H. Speleers, Hierarchical spline spaces: Quasi-interpolants and local approximation estimates, *Adv. Comput. Math.* **43** (2017) 235–255.
35. R. Stevenson, The completion of locally refined simplicial partitions created by bisection, *Math. Comp.* **77** (2008) 227–241.
36. A. Veeser and R. Verfürth, Explicit upper bounds for dual norms of residuals, *SIAM J. Numer. Anal.* **47** (2009) 2387–2405.
37. R. Verfürth, *A Posteriori Error Estimation Techniques for Finite Element Methods* (Oxford Univ. Press, 2013).
38. A.-V. Vuong, C. Giannelli, B. Jüttler and B. Simeon, A hierarchical approach to adaptive local refinement in isogeometric analysis, *Comput. Methods Appl. Mech. Eng.* **200** (2011) 3554–3567.